Ab Initio Parametrized MM3 Force Field for the Metal-Organic Framework MOF-5

MAXIM TAFIPOLSKY, SAEED AMIRJALAYER, ROCHUS SCHMID
Lehrstuhl für Anorganische Chemie 2, Organometallics and Materials Chemistry, Ruhr-Universität Bochum, Universitätsstr. 150, D-44780 Bochum, Germany

Received 3 May 2006; Accepted 13 July 2006
DOI 10.1002/jcc.20648
Published online 14 February 2007 in Wiley InterScience (www.interscience.wiley.com).

Abstract: A new valence force field has been developed and validated for a particular class of coordination polymers known as nanoporous metal-organic frameworks (MOFs), introduced recently by the group of Yaghi. The experimental, structural, and spectroscopic data in combination with density functional theory calculations on several model systems were used to parametrize the bonded terms of the force field, which explicitly treats the metal–oxygen interactions as partially covalent as well as distinguishes different types of oxygens in the framework. Both the experimental crystal structure of MOF-5 and vibrational infrared spectrum are reproduced reasonably well. The proposed force field is believed to be useful in atomistic simulations of adsorption/diffusion of guest molecules inside the flexible pores of this important class of MOF materials.

 J Comput Chem 28: 1169–1176, 2007

Key words: force field; parametrization; metal-organic framework; MM3; molecular dynamics

Introduction

Molecular simulations using classical potential models had and still have a strong impact on the research of meso-, micro- and nanoporous materials such as zeolites (for some recent studies, see Ref. 1). Detailed investigations of diffusion and adsorption of molecules within the pores helped to understand the transport and binding mechanisms on a microscopic level. Recently, a new class of nanoporous materials has been developed, based on the self assembly of metal-oxide clusters linked together with a variety of polyatomic organic bridging ligands, the so-called metal-organic frameworks (MOF).[2–5] Like zeolites, MOFs are characterized by high and tunable surface areas, thus permitting to use them as efficient storage materials as well as for separation processes and in catalysis.[6,7] Rational design of the properties of such materials can be greatly facilitated by molecular dynamics (MD) and Monte-Carlo (MC) classical simulations.[8,9] Therefore, there is a need for a practical procedure to develope a realistic force field which can capture the main interactions within the simulated guest–host system. Furthermore, to reliably describe both the lattice dynamics and diffusion/adsorption properties of a guest molecule inside the porous material, it is important to treat the host lattice (MOF) as nonrigid. Experience accumulated from the zeolite modeling is of great help here.

Recently, several molecular simulations have been performed, concentrating mainly on the adsorption properties of various MOFs and on diffusion inside these new materials corroborating available experimental findings with different success.[10–14] In most of these studies, to the best of our knowledge, MOFs have been modeled as rigid frameworks, with the atoms held fixed in their experimentally determined crystallographic positions. In these studies, either a generic all-atom based force field, such as UFF and DREIDING, or a standard diagonal force field like CVFF have been used. Only the nonbonding parameters, describing the pairwise interactions between the guest and the host atoms of the particular force field, have been utilized. Partly, they have been refined to match experimental data (such as adsorption isotherms), or using first principles calculations.[14–17] It can be anticipated, however, that, at low loadings, the use of a flexible framework is crucial for predicting transport properties of small guest molecules in MOFs properly, since, in this case, the self-diffusivities are dominated by adsorbate–host collisions. This is even more relevant for larger guests, which fit tightly in the MOF pores, forcing the metal-organic framework to deform in order to allow a migration from cage to cage. Since we are interested in the simulation of large chemical vapour deposition (CVD) type precursor molecules for the synthesis of "Metal@MOF" type systems targeted on catalysis,[18] this is an important issue. In fact, it was recently shown experimentally that

Correspondence to: R. Schmid; e-mail: rochus.schmid@rub.de

Contract/grant sponsor: Alfried Krupp von Bohlen und Halbach Stiftung
Contract/grant sponsor: Deutsche Forschungsgemeinschaft; contract/grant number: (SPP 1119)

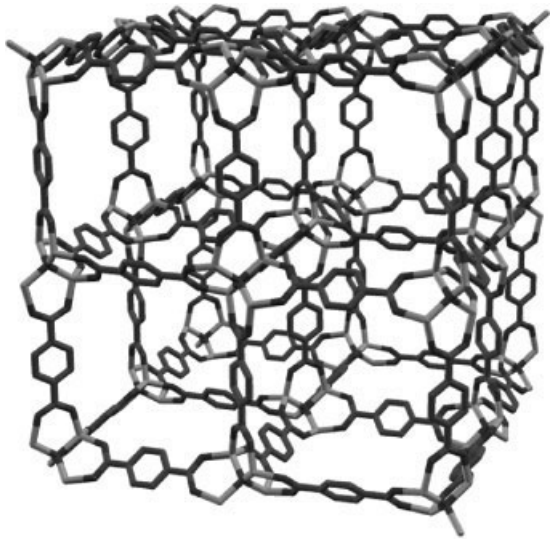

Figure 1. The structure of the MOF-5 with eight cubic pores. Zinc, oxygen, and carbon atoms are shown in grayscale from light (zinc) to dark (oxygen). Hydrogens are omitted for clarity.

an MOF, fully loaded with ferrocene molecules, becomes strongly deformed.[19] Furthermore, flexible frameworks are essential for the simulation of chemical reactions inside the host, because the energy exchange between reactants or products and the heat bath of the framework should be accounted for. Experience gained from the adsorption/diffusion modeling in zeolites underscores the need for potential models that include lattice flexibility, especially when the sorbates are tightly fitting the pores.[20–22] For example, lattice flexibility was found to have a very strong influence on the diffusivity of benzene in silicalite.[23]

In this article, we describe the parametrization of an all-atom empirical force field based on density functional theory (DFT) calculations on the nonperiodic model systems with the aim to be able to treat the full periodic metal-organic framework, known as MOF-5,[24] with the flexible host lattice. We validate our empirical potential by its ability to reproduce both the geometrical parameters of the calculated reference model structures and known experimental data together with their vibrational normal modes as well.

MOF-5 is composed from Zn_4O clusters linked together by 1,4-benzenedicarboxylate (BDC) moieties such that the resulting framework with formula unit $Zn_4O(BDC)_3$ consists of cubic pores, where BDC forms the edges of the cubes and the Zn_4O clusters form the vertexes. In half of the pores, of width about 13 Å each, the face of the carbon rings points toward the center of the pore, and in the remaining pores, the edges of the carbon rings face the center (Fig. 1).

A tetranuclear zinc benzoate, $Zn_4O(O_2CC_6H_5)_6$, was used as a model system (Fig. 2). The structure of this compound has been the subject of several X-ray single crystal studies.[25,26] In addition, it was characterized by infrared and mass spectroscopies.[25] This molecule is small enough to be amenable to ab initio calculations but, at the same time, it represents the most salient features of periodic MOF-5.

One can anticipate that the torsional motion of the phenylene moiety should influence to a large extent the transport properties of guest molecules which tightly fit the pores in MOF-5. Therefore, it is very important for the force field parametrization to evaluate its barrier to internal rotation reliably. To this end, we have performed additional calculations on another model system $Zn_4O(O_2CH)_5$—BDC—$Zn_4O(O_2CH)_5$ (Fig. 3), mimicking one edge of the unit cell of MOF-5.

Our goal here is to obtain a force field that can reliably predict the structure and dynamic properties of MOF-5 and is able to simulate transport properties of simple guest molecules inside the MOF-5.

Computational Details

The molecular structures for our model systems were fully optimized by DFT calculations using the hybrid functional, B3LYP.[27–29] The B3LYP method was chosen due to its success in structural prediction. Both the Stuttgart effective relativistic small core potential[30] (basis set I) and all-electron 6-31G(d,p) basis sets (basis set II) were employed for the Zn atom, whereas the 6-31G(d,p) basis set was used for the C, O, and H atoms.[31] Additional calculations were performed for the $Zn_4O(O_2CC_6H_5)_6$ complex with an all-electron triple-zeta valence basis set, (TZVPP), of Ahlrichs et al.,[32] supplemented with the polarization functions on all atoms (basis set III). For smaller model systems, a series of the correlation consistent all-electron basis sets of Dunning and coworkers (cc-pVXZ; X = D,T,Q)[33] were employed. The second order Møller–Plesset theory (MP2)[34] and the coupled cluster theory considering single, double, and quasiperturbative triple excitations, CCSD(T),[35–37] were used in some single-point calculations on smaller model systems (at geometries optimized at the DFT level) to get more reliable energy estimates. The CCSD(T) method was selected because of its well-established reliability in accurate molecular property prediction. All calculations were carried out with the Gaussian program

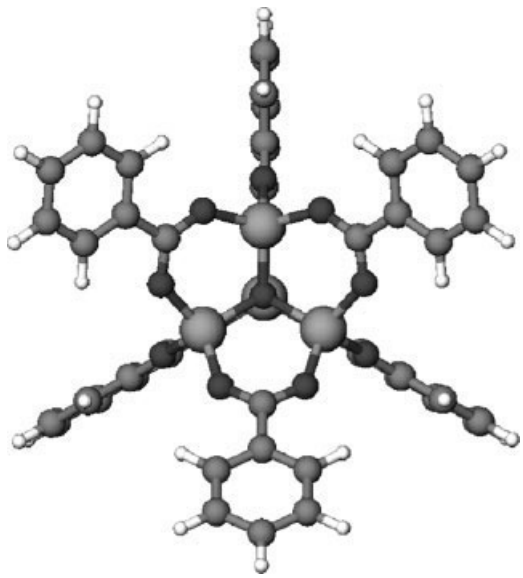

Figure 2. Molecular structure of $Zn_4O(O_2CC_6H_5)_6$. Zinc and carbon atoms are shown as large and small gray balls, respectively; oxygens are shown as small dark gray balls.

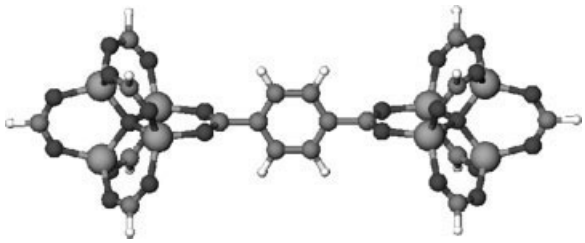

Figure 3. Molecular structure of $Zn_4O(O_2CH)_5$—BDC—$Zn_4O(O_2CH)_5$. The perpendicular orientation of the C_6H_4 unit with respect to the OCO planes is shown. Zinc and carbon atoms are shown as large and small gray balls, respectively, and oxygens are shown as small dark gray balls.

package.[31] Because of the presence of low vibrational modes (on the order of 10 cm^{-1}), we used, in all DFT calculations, a more tight convergence criterion (Opt = Tight) and a finer grid for the integration (Int = Ultrafine). Both the Gaussian[31] and Molden[38] version 4.4 program packages were used for the calculation of electrostatic potentials and for fitting the point charges (a locally modified version of the Molden program was used). For MD simulations, the TINKER program package[39] was used.

Results and Discussion

Reference Systems

The optimized geometry for the $Zn_4O(O_2CC_6H_5)_6$ model system of T_d symmetry was confirmed to be a true minimum by vibrational frequency calculations. The calculated structural parameters are compared with the experimental results in Table 1. To our knowledge, two X-ray single crystal structure determinations are available in the literature.[25,26] Clegg et al.[25] reported the crystal structure with one solvent molecule (acetone) per one $Zn_4O(O_2CC_6H_5)_6$ complex, whereas Yin et al.[26] was able to refine a crystal structure for a pure tetranuclear zinc benzoate but with a much larger unit cell. As can be seen from Table 1, the Zn—O bond distances from both X-ray studies are quite similar to each other. We note that the calculated values overestimate the experimental ones (on average). Interestingly, the B3LYP method along with the basis set I predicts the bond distance between the central O atom (O_{cent}) and the Zn atom to be slightly shorter (0.003 Å) than that between the carboxylate oxygen (O_{carb}) and Zn, whereas the opposite is true with the basis set II. We note that the calculated C—O and C—C bond distances are very close to the experimental ones, thus justifying the use of modest 6-31G(d,p) basis sets for the light elements.

In a recent work,[40] Braga and Longo have calculated the molecular structure of tetranuclear zinc acetate, $Zn_4O(O_2CCH_3)_6$, by both semiempirical (AM1 and PM3) and ab initio methods. They found that the Zn—O_{cent} bond is longer than the Zn—O_{carb} bond both at the Hartree-Fock (HF/6-31G(d,p); r(Zn—O_{cent}) = 1.980 Å, r(Zn—O_{carb}) = 1.966 Å) and DFT level (B3LYP/6-31G(d,p); r(Zn—O_{cent}) = 1.956 Å, r(Zn—O_{carb}) = 1.950 Å), for the latter method the difference being significantly smaller (0.014 vs. 0.006 Å). These results can be compared with ours (see Table 1) obtained for $Zn_4O(O_2CC_6H_5)_6$ at the B3LYP/II level with the same all-electron basis set. Only semiempirical (AM1 and PM3) calculations were performed there on the $Zn_4O(O_2CC_6H_5)_6$ molecule with the conclusion that the PM3 results were overall in better agreement with the experimental X-ray data than the AM1 results despite the fact that the AM1 method described better the torsional motion of the phenyl moiety in $Zn_4O(O_2CC_6H_5)_6$.

Since we are interested in a reliable force field able to describe MOF-5 lattice dynamics, the method, chosen for the parametrization, should itself reproduce the experimental vibrational frequencies as close as possible. Since experimental vibrational data for $Zn_4O(O_2CC_6H_5)_6$ are restricted to the range 1400–1750 cm^{-1},[25] the spectral data in the 200–600 cm^{-1} region for some tetranuclear zinc complexes, $Zn_4O(O_2CR)_6$ (R = CH_3, $C(CH_3)_3$),[41,42] can be used instead to access the reliability of a theoretical method used. This region is characterized by the vibrational modes mainly due to the $Zn_4O(O_2C)_6$ moiety. The calculated frequency of 534 cm^{-1} (B3LYP/6-31G(d,p)) for the asymmetric vibration of the central oxygen atom (t_2 in T_d symmetry) is very close to the experimental one (530 cm^{-1}), whereas symmetric stretching of the Zn_4O tetrahedron (a_1) is predicted to be at 268 cm^{-1}, which slightly overestimates the experimental value (225 cm^{-1}). It has been shown that the relatively strong feature at 530 cm^{-1} is due solely to the movement of the central oxygen atom in a rigid cage of zinc atoms and is very characteristic of these complexes.[42] This fact is corroborated by our calculations. At the same time, we found that the vibrational frequency for the symmetric stretching of the Zn_4O tetrahedron, which is inactive in the infrared but very strong in the Raman,[41] depends on the substituent R. Our additional calculations with R = CH_3 gave the value of 210 cm^{-1} for this symmetric stretching mode. The symmetric stretchings of the bonds between the zinc and the oxygens of the carboxylate linker are found at 495 (t_2), 499 (e), and 504 (a_1) cm^{-1}, whereas the values of 609 (t_1) and 619 (t_2) cm^{-1} correspond to the asymmetric stretching of the same bonds. We note that the vibrational frequencies for these motions are also very sensitive to the substituent R and may vary in a wide range. Our additional calculations on the $Zn_4O(O_2CCH_3)_6$ complex gave the values in the 330–350 cm^{-1} region which is in agreement with the assignment proposed by Johnson et al.,[41] who identified the bands at 336 cm^{-1} (infrared) and at 342 cm^{-1} (Raman), respectively, with asymmetric and symmetric stretchings of the bonds between the zinc and the oxygens of the acetate linker. Braga and Longo[40] have tentatively assigned a strong feature at 442 cm^{-1}, measured in the infrared spectrum of $Zn_4O(O_2CC(CH_3)_3)_6$ by Berkesi et al.,[42] to asymmetric stretchings of these bonds, whereas their calculations (HF/6-31G(d,p)) on the $Zn_4O(O_2CCH_3)_6$ complex gave a value of 362 cm^{-1}.

Table 1. Selected Bond Distances (in Å) for $Zn_4O(O_2CC_6H_5)_6$.

Method	Zn—O_{cent}	Zn—O_{carb}	C_{carb}—O_{carb}	C_{carb}—C_{ph}
B3LYP/I	1.969	1.972	1.272	1.495
B3LYP/II	1.953	1.948	1.271	1.493
B3LYP/III	1.975	1.973	1.264	1.494
X-ray [25]	1.933–1.945	1.937–1.969	1.244–1.267	1.488–1.501
X-ray [26]	1.936–1.950	1.930–1.950	1.234–1.270	na

The symmetric and asymmetric stretchings of the carboxylate group correspond to the most strong bands in the 1400–1750 cm^{-1} region of the infrared spectra of the basic zinc benzoate, $Zn_4O(O_2CC_6H_5)_6$. The solid-state spectra show a broad line at 1410 cm^{-1} and a strong line at 1562 cm^{-1}, which Clegg et al.[25] assigned to the symmetric and asymmetric stretchings, respectively. In chloroform solution of the basic zinc benzoate, they observed two strong bands at 1570 and 1607 cm^{-1} and assigned them to asymmetric stretchings of the carboxylate group. At the same time, the band due to symmetric stretchings was shifted in solution only slightly to 1417 cm^{-1}. Our calculations (B3LYP/I) gave the values of 1442, 1445, and 1467 $cm^{-1}$for symmetric stretchings and of 1582 and 1668 cm^{-1} for the asymmetric stretchings. The calculated infrared spectrum is dominated by the two strong lines at 1445 and 1668 cm^{-1}.

Overall, the two basis sets (I and II), employed in the present work, gave very similar results and are in good agreement with experimental findings, both structural and vibrational, and, hence, we are confident that our chosen method, B3LYP/I, is adequate for the force field parametrization.

We have optimized the geometry for another model system, $Zn_4O(O_2CH)_5$—BDC—$Zn_4O(O_2CH)_5$ (Fig. 3) both at the B3LYP/I and B3LYP/II levels. The influence of the phenylene ring on the difference between the Zn—O_{cent} and Zn—O_{carb} bond lengths is quite significant. We found that the Zn—O_{cent} is about 0.01 (B3LYP/I) and 0.02(B3LYP/II) Å longer than the Zn—O_{carb} bond. Our DFT calculations at the B3LYP/II level give the following values for the Zn—O bond distances (B3LYP/I results in parentheses): r(Zn—O_{cent}) = 1.962 (1.978) Å, r(Zn—O_{carb}) = 1.942 (1.968) Å. Although the difference in the experimental Zn—O_{cent} and Zn—O_{carb} bond distances for the fully desolvated MOF-5[24] is reproduced by DFT calculations, the absolute values are systematically longer by 0.01–0.03 Å when compared with the experimental ones (r(Zn—O_{cent}) = 1.9498 Å, r(Zn—O_{carb}) = 1.9378 Å).

The estimated barrier to internal rotation of 15 kcal/mol (B3LYP/I) is the energy difference between the fully optimized planar and perpendicular (shown in Fig. 3) orientations of the C_6H_4 unit with respect to the OCO planes. The planar configuration of D_{2h} symmetry was confirmed to be a true minimum, whereas the perpendicular one of the same symmetry was a second-order saddle point with two imaginary frequencies corresponding to this particular torsional motion. These torsional frequencies are calculated to be in the range of 60–80 cm^{-1}. Frequency calculations give the difference in zero-point vibrational energies of about 1 kcal/mol. We should note that rotational barriers of molecules comprised of a benzene ring and a π-conjugated substituent, such as terephthalic acid anion, pose a challenge for theoretical methods (see, for example, Ref. 43). We investigated the influence of both the level of theory and basis set on this barrier. To this end, we have carried out higher level calculations on a simpler model system, dilithium terephthalate, which was used previously in a different context.[16,44] Three methods, B3LYP, MP2, and CCSD(T) were used along with the correlation consistent cc-pVXZ (X = D,T,Q) basis sets. Our results indicate that the energy difference between the fully optimized planar and perpendicular orientations (D_{2h} symmetry) depends somewhat on the basis set used and the level of theory employed amounting to the values (kcal/mol) of 16.1 (B3LYP/cc-pVDZ), 14.1 (B3LYP/cc-pVTZ), 13.5 (B3LYP/cc-pVQZ) kcal/mol, 15.7 (MP2/cc-pVDZ), 15.8 (CCSD(T)/cc-pVDZ), and 14.1 (MP2/cc-pVTZ). Thus, we are confident that our estimated torsional barrier for use in the force field parametrization of MOF-5 is quite reliable within 1 kcal/mol.

The effective atomic charges were obtained for two of our model systems, $Zn_4O(O_2CC_6H_5)_6$ and $Zn_4O(O_2CH)_5$—BDC—$Zn_4O(O_2CH)_5$ (Figs. 2 and 3) by fitting to the calculated electrostatic potential. Since both B3LYP/I and B3LYP/II levels gave similar values, we discuss the results based on the B3LYP/I calculations. The charge distribution in the $Zn_4O(O_2C)_6$ unit in these two model systems was found to be very similar. For the $Zn_4O(O_2CC_6H_5)_6$ complex, several sampling schemes (such as MK,[45] CHelpG,[46] OPEP version 1.0; A locally modified version of the OPEP program was used[47]) were employed to investigate the sensitivity of the resulting effective charges. The same set of van der Waals radii was used throughout (in Å): Zn: 2.29, O: 1.40, C: 1.50, H: 1.20. Convergence of the values was checked by comparing the charges on the symmetry equivalent atomic sites. We use a much higher point density than the default in the Gaussian program as was recommended in a careful study by Sigfridsson and Ryde.[48] We found that about 1900 grid points per atom was sufficient to produce converged charges. Also, both the true electrostatic potential and that based on the distributed multipole representation[38,49] were tried. Since the van der Waals radii were used to construct the surfaces, on which the electrostatic potential is evaluated, the influence of the Zn radius in the range 1.0–2.3 Å on the resulting charges was also explored and found to be not very critical. The value of 2.29 Å, as recommended in,[50] was adopted. Overall, the effective charge on the Zn atom was found in the range 1.3–1.7 e depending on the sampling scheme and method of representation of the electrostatic potential, whereas the effective charge on the central oxygen atom (O_{cent}) changed in a more wide range from −1.1 to −2.0 e. These findings are not unexpected since the difficulty in assigning the potential-derived charges to buried atoms (such as O_{cent}) is well documented (see, for example, Ref. 51). The atomic charges in both the phenylene (C_{ph} and H) and carboxylate (C_{carb} and O_{carb}) moieties are found to be quite reproducible. To estimate a possible range of variations of the partial charges, a statistical analysis developed by Millot et al.[47] can be very instructive here. The distribution functions were obtained from 1,000,000 trials from a set of about 17,000 grid points. The electrostatic potential was calculated at points selected to be within a shell between 2.0 and 2.5 times the van der Waals surface of the molecule with the grid spacing of 0.4 Å. The root mean square deviation between the true electrostatic potential and its point charge-derived approximation did not exceed 1 kcal/mol. The conservation of the molecular charge constraint was not imposed and the absolute residual charge was less than 0.004 e. The reliability of the charge distribution analysis was judged on the basis of the resulting molecular moments: the dipoles and octupoles vanished exactly (because of D_{2h} symmetry), and the values for the quadrupole and hexadecapole moments were qualitatively in agreement with the results from the DFT calculations. Figure 4 shows the probability distribution functions of partial charges for symmetrically nonequivalent atoms for $Zn_4O(O_2CH)_5$—BDC—$Zn_4O(O_2CH)_5$. It is clearly seen from this figure that the charge on the central oxygen atom is ill-defined, exhibiting large variations from its most probable value. On the other hand, the distributions of partial charges on the C_{carb} and O_{carb} atoms are quite narrow, meaning that the values can be assigned reliably to these atoms.

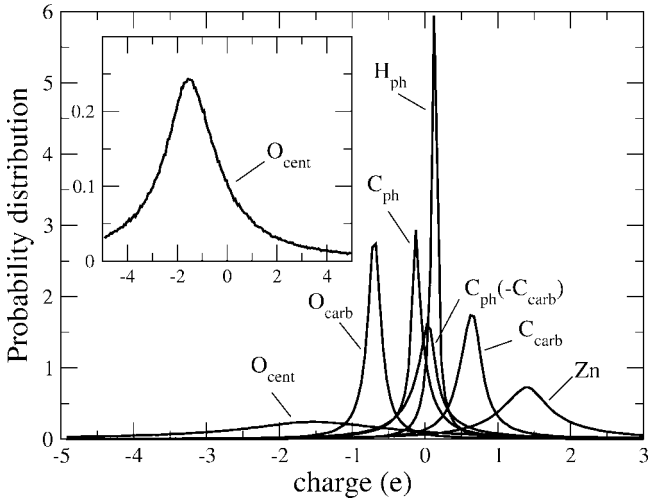

Figure 4. Probability distributions of partial charges for symmetrically nonequivalent atoms in $Zn_4O(O_2CH)_5$—BDC—$Zn_4O(O_2CH)_5$. The inset shows the distribution of charge for the O_{cent} atom in more detail (note the change in the scale of the vertical axis).

Our results are in reasonable agreement with those obtained recently by DFT calculations at the PBE/6-31G+G(d) level of Sagara et al.[16] for the $Zn_4O(O_2CCH_3)_5$—BDC—$Zn_4O(O_2CCH_3)_5$ model system using the CHelpG[46] sampling method.

We adopted the results from the Merz–Kollman sampling scheme[45] as our final set of effective charges, since this method was found previously to be superior.[48] The partial charges for symmetrically independent atoms used in the force field parametrization are listed in Table 2.

Parametrization

We adopted a similar strategy for a force field parametrization used previously for zeolite modeling by Ermoshin et al.[52] The results of our DFT calculations (B3LYP/I) on the $Zn_4O(O_2CC_6H_5)_6$ complex were used as reference. The Hessian matrix (second derivatives of the energy) in Cartesian coordinates was transformed to a set of force constants in (redundant) internal coordinates with the translational and rotational motions projected out. We used a locally modified version of the program written by Sipachev.[53] The MM3(2000) force field of Allinger et al.[54] was used as implemented in TINKER.[39] The metal–oxygen interactions were treated as partially covalent. Four new atomic types have been introduced: four-coordinated zinc and central oxygen (O_{cent}) atoms, two- and three-coordinated oxygen (O_{carb}) and carbon (C_{carb}) atoms, respectively, of the carboxylate group. The diagonal force field parameters for the $Zn_4O(O_2C)_6$ unit augmented the parameters of the phenylene moiety, where the original MM3 atom types 2 and 5 were used for the carbon (C_{ph}) and hydrogen atoms, respectively. As suggested by Allinger et al.,[55] in order to take the conjugation in the phenylene moiety into account, we adjusted the values for the C_{ph}—C_{ph} bond stretching and the corresponding reference bond length together with the twofold torsional parameters for the rotation around C_{ph}—C_{ph} bonds by performing a self-consistent field molecular orbital calculation for the π-system using a modified Pariser–Parr–Pople method as implemented in TINKER. The reference values for the Zn—O bond lengths were tuned to match the experimental values, since our DFT calculations overestimated these bond distances (see earlier). The off-diagonal terms representing coupling interactions between internal coordinates for the $Zn_4O(O_2C)_6$ unit were ignored in the present work except for the stretch-bend term describing the Zn—O_{cent}/Zn—O_{cent}—Zn interaction which was deemed necessary to reproduce the asymmetric stretch of the Zn_4O tetrahedron at about 530 cm^{-1} (see earlier). Also, both the stretch-bend and bend-bend terms of the original MM3 atom type 3 were retained for our new type carboxylic carbon atom without reoptimization. The van der Waals parameters for the Zn atom were taken from Ref. 50, and those for the newly introduced carbon and oxygen atom types were assigned the same values as in the original MM3 force field. The long-range Coulomb interactions were described via bond dipoles using effective atomic charges obtained as described earlier. To describe the torsional potential of the phenylene group, we used a single cosine term of the form $V(\varphi) = 1/2V_0(1 - \cos(2\varphi))$, where φ is the C_{ph}—C_{ph}—C_{carb}—O_{carb} dihedral angle and the parameter V_0 was adjusted to reproduce the barrier to internal rotation of the phenylene moiety as obtained by our DFT calculations (see earlier). The remaining torsional potentials in the $Zn_4O(O_2C)$ unit were approximated by a single cosine term of the same form $V(\varphi) = 1/2V_0(1 - \cos(2\varphi))$.

Initial force constants from the Hessian transformation were subjected to a fine tuning procedure (mainly torsional parameters) with the help of AFMM tool,[56] which was interfaced with the TINKER program. Here, special care has been taken to reproduce the low frequency deformation modes in the model system, $Zn_4O(O_2CC_6H_5)_6$. This is important for a realistic simulation of the lattice deformations of MOF-5. We interfaced our program for the normal-coordinate analysis and Hessian transformations with the TINKER vibrational module (VIBRATE) where the numerical derivatives were employed in the frequency calculations. Our final parameters are listed in Table 3.

As a result, we can reproduce the calculated (DFT) vibrational frequencies for the $Zn_4O(O_2C)$ core in our model systems. Some selected vibrational modes are compared in Table 4. Note that the remaining discrepancies are mainly due to the fact that we did not parameterize cross terms (with the exception of the central oxygen atom). The calculated barrier to internal rotation of the phenylene group in the model system $Zn_4O(O_2CH)_5$—BDC—$Zn_4O(O_2CH)_5$ is also reproduced by the force field.

Table 2. Atomic Charges Used in the Force Field Parameterization.

Atom	Charge (e)
O_{cent}	−1.44
Zn	1.26
O_{carb}	−0.67
C_{carb}	0.68
C_{ph}(—C_{carb})	0.06
C_{ph}	−0.16
H	0.16

Table 3. Additional Force Field Parameters for MOF-5.

Bond stretches		
Atom types	Reference distance (Å)	Force parameter (mdyn/Å)
$Zn—O_{cent}$	2.075	0.85
$Zn—O_{carb}$	2.015	0.85
$C_{carb}—O_{carb}$	1.285	7.54
$C_{carb}—C_{ph}$	1.480	4.84
$C_{ph}—C_{ph}$	1.38	6.56
	In-plane angle bending	
	Reference angle (degree)	Force parameter (mdyn Å/rad^2)
$Zn—O_{cent}—Zn$	109.471	0.40
$O_{cent}—Zn—O_{carb}$	111.3	0.30
$O_{carb}—Zn—O_{carb}$	107.6	0.22
$Zn—O_{carb}—C_{carb}$	131.2	0.43
$O_{carb}—C_{carb}—O_{carb}$	125.5	0.64
$C_{ph}—C_{ph}—C_{carb}$	120.0	0.73
$O_{carb}—C_{carb}—C_{ph}$	117.0	0.78
	Out-of-plane angle bending	
	Reference angle (degree)	Force parameter (mdyn Å/rad^2)
$(O_{carb},O_{carb})C_{carb}—C_{ph}$	0.0	0.46
Stretch-bend (mdyn/rad)		
$Zn—O_{cent}/Zn—O_{cent}—Zn$	0.4	
	Torsional parameters	
	V_0 (kcal/mol)	
$C_{ph}—C_{ph}—C_{carb}—O_{carb}$	2.0	
$O_{cent}—Zn—O_{carb}—C_{carb}$	10.0	
$Zn—O_{cent}—Zn—O_{carb}$	10.0	
$Zn—O_{carb}—C_{carb}—O_{carb}$	10.0	
$Zn—O_{carb}—C_{carb}—C_{ph}$	10.0	
	Bond dipoles (D)	
$Zn—O_{cent}$	3.352	
$Zn—O_{carb}$	2.794	
$C_{carb}—O_{carb}$	2.255	
$C_{carb}—C_{ph}$	−0.432	
$C_{ph}—H$	−0.6	
	van der Waals parameters	
	Radius (Å)	ε (kcal/mol)
Zn	2.29	0.276
O	1.82	0.059
C	1.94	0.056
H	1.62	0.020

Validation and Application

In general, by parametrizing a force field one seeks to make structural or energetic predictions beyond the training set. In our case, the training set consisted of two nonperiodic systems, representing a corner and an edge of the periodic cubic MOF-5 structure. Note that no experimental data from the periodic framework has been used in the parametrization. In this section, we will present first basic structural and dynamic results, calculated for MOF-5 with the valence force field developed in the present work.

The experimentally determined structure of the periodic MOF-5 is well reproduced by the force field. The lattice constant of 25.9457 Å obtained from the geometry optimization of periodic MOF-5 using this force field is in agreement with the experimental value (25.8849 Å) obtained for the fully desolvated MOF-5.[24] Both the unit cell volume and the atomic coordinates were optimized simultaneously with the XTALMIN program of the TINKER package. For the simulations, a cubic box containing 424 atoms was used. In the periodic energy minimizations, a cutoff value of 12.0 Å was used to evaluate the van der Waals interactions, while the electrostatic interactions were calculated exactly by Ewald summation. The root mean square gradient at convergence was set to 0.001 kcal/mol/Å. We can compare the lattice constant resulting from our periodic molecular mechanics calculations with those obtained previously by several periodic ab initio DFT calculations. Fuentes–Cabrera et al. reported the value of 25.6141 Å based on the local-density approximation to DFT and a plane wave basis set.[57] This level of theory underestimates the Zn—O bond distances by about 0.03 Å when compared with the experimental data. Recently, Mattesini et al. arrived at the value of 25.888 Å in their local-density DFT calculation using localized numerical basis functions.[58] On the other hand, Mueller and Ceder, using the gradient corrected correlation functional, PBE, in combination with plane waves, obtained a somewhat longer Zn—O bond distances (0.02 Å) and slightly overestimated the lattice constant (26.137 Å).[59] Interestingly, Sagara et al. reported the value of 25.77 Å based on the

Table 4. Selected Vibrational Modes for the $Zn_4O(O_2C)$ Core (in cm^{-1}).

Mode	B3LYP/I	Force field
	$Zn_4O(O_2CC_6H_5)_6$	
$\nu_s(Zn—O_{cent})$	268	260
$\nu_{as}(Zn—O_{cent})$	524	531
$\nu_s(Zn—O_{carb})$	490–497	473–482
$\nu_{as}(Zn—O_{carb})$	605–611	569
$\nu_s(C_{carb}—O_{carb})$	1442, 1445, 1467	1407–1409
$\nu_{as}(C_{carb}—O_{carb})$	1582, 1668	1693
	$Zn_4O(O_2CH)_5—BDC—Zn_4O(O_2CH)_5$	
$\nu_s(Zn—O_{cent})$,in-phase	230	213
$\nu_s(Zn—O_{cent})$,out-of-phase	218	200
$\nu_{as}(Zn—O_{cent})$	512–516	516–530
$\nu_s(Zn—O_{carb})$,in-phase[a]	466	452
$\nu_s(Zn—O_{carb})$,out-of-phase[a]	578	541
$\nu_{as}(Zn—O_{carb})$,in-phase[a]	599	576
$\nu_{as}(Zn—O_{carb})$,out-of-phase[a]	624	572

[a]The in-phase and out-of-phase vibrational modes correspond to the stretching of the $Zn—O_{carb}$ bonds linked by the phenylene group.

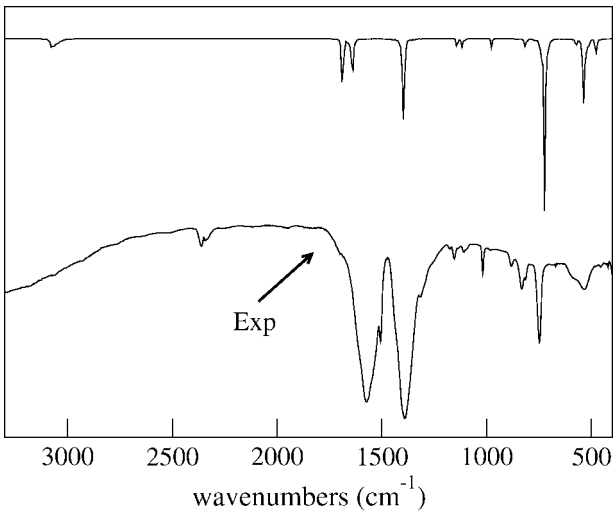

Figure 5. Comparison of the calculated (top) and measured (bottom) infrared spectrum of MOF-5 at 300 K. The shoulder at high wavenumbers and the peak above 2300 cm^{-1} in the experimental spectrum are due to water and CO_2.

periodic optimization with the same gradient corrected correlation functional, but with the 6-31G(d) basis set.[16] Mulder et al. reported a value of 25.8399 Å using plane waves and generalized gradient approximation to DFT (unfortunately, not specified).[60] Again, using Gaussian type basis functions but with the hybrid functional B3LYP, Civalleri et al. calculated a lattice parameter of 26.088 Å.[61] We conclude that our force field calculations give reliable estimates of the unit cell dimensions of periodic MOF-5 when compared with experiment and other theoretical methods.

In addition, we have also calculated the infrared spectrum of the periodic MOF-5 from a classical MD simulation, using the dipole moment time derivative autocorrelation function,[62] which is shown in Figure 5 together with the observed one.[63] Initially, the energy minimization of MOF-5 was performed. Then, the system was subjected to 100 ps of temperature equilibration at 300 K, followed by 150 ps of unrestrained MD collection run using the NVE ensemble with the time step of 1 fs. The IR spectrum was calculated from the last 50 ps of MD trajectory using the dipole moment time derivative autocorrelation function. A local version of the program written by H. Forbert with a contribution from A. Kohlmeyer was used to calculate the power spectrum. The frequency step in the simulated spectra was 10 cm^{-1}. The effective point charges were evaluated from bond dipole moments and bond lengths. We note that the most characteristic features of the observed spectrum are well reproduced. The most intense absorptions due to asymmetric and symmetric C_{carb}—O_{carb} stretchings around 1690 and 1400 cm^{-1} are very similar to the values calculated for the model systems (see Table 4), as well as to the ones calculated by DFT (B3LYP level) for the periodic MOF-5.[61]

The energy for distortion from the cubic lattice has been calculated both for a monoclinic ($\alpha < 90$; $\beta = \gamma = 90$) and a triclinic deformation ($\alpha = \beta = \gamma < 90$). A harmonic fit gave force constants of 0.437 and 1.29 kcal/mol/deg^2, respectively. By an unconstrained optimization of structure and all lattice parameters, the cubic structure is recovered. Thus, as expected, MOF-5 is very rigid with respect to a collapse of the lattice, which explains its high stability and the fact that all solvent can be removed.

Apart from the theoretical prediction of the properties of the material itself, we have also performed MD simulations of the diffusion of benzene molecules in the porous material, focusing on the effect of lattice flexibility. Here, the application of our force-field can be seen as a means to bridge the time scale problem, prohibiting the use of first principles methods for long term simulations. Note that for this particular purpose, the reproduction of the training set is completely sufficient. The calculated self-diffusion coefficient D_{self} at room temperature $(2.5(3) \times 10^{-9}\ m^2/s)$ is in good agreement with the experimental value $(2.0 \times 10^{-9}\ m^2/s)$,[64] when lattice flexibility is taken into account, whereas it is significantly (by roughly an order of magnitude) overestimated using the rigid lattice $(19(2) \times 10^{-9}\ m^2/s)$. Thus, a correlated motion of the framework and the guest molecules leads to an unexpected reduction of the mobility, in contrast to the usual findings for zeolites.[21] Details of this application are published elsewhere.[65] Note that our findings are also in accord with the results of Mattesini et al.,[58] who obtained a relatively low value for the Debye temperature of the cubic MOF-5 crystal (294.62 K), based on first-principles calculations, indicating the lattice to be rather flexible.

Conclusion

A simple procedure has been developed to parametrize the force field for a particular class of metal-organic framework materials, MOF-5. The present force field can be easily extended by including the off-diagonal parameters as well as by adding a more realistic treatment of the long-range Coulomb interactions via distributed atomic multipoles, thus going beyond the point charge model. Work along these lines is in progress.

Acknowledgment

We thank Prof. Roland A. Fischer for stimulating discussions and his support.

References

1. Demontis, P.; Suffritti, G. B. Chem Rev 1997, 97, 2845.
2. Rowsell, J. L. C.; Yaghi, O. M. Micropor Mesopor Mater 2004, 73, 3.
3. Janiak, C. Dalton Trans 2003, 2781.
4. James, S. L. Chem Soc Rev 2003, 32, 276.
5. Kitagawa, S.; Noro, S.-I.; Nakamura, T. Chem Commun 2006, 701.
6. Mueller, U.; Schubert, M.; Teich, F.; Puetter, H.; Schierle-Arndt, K.; Pastre, J. J Mater Chem 2006, 16, 626.
7. Panella, B.; Hirscher, M. Adv Mater 2005, 17, 538.
8. Allen, M. P.; Tildesley, D. J. Computer Simulation of Liquids; Oxford Science: Oxford, 1989.
9. Frenkel, D.; Smit, B. Understanding Molecular Simulation: From Algorithms to Applications, 2nd ed., Academic Press: Boston, 2002.
10. Vishnyakov, A.; Ravikovitch, P. I.; Neimark, A. V.; Bulow, M.; Wang, Q. M. Nano Lett 2003, 3, 713.
11. Sarkisov, L.; Duren, T.; Snurr, R. Q. Mol Phys 2004, 102, 211.
12. Sagara, T.; Ortony, J.; Ganz, E. J Chem Phys 2005, 123, 214707.
13. Skoulidas, A. I.; Sholl, D. S. J Phys Chem B 2005, 109, 15760.

14. Yang, Q. Y.; Zhong, C. L. J Phys Chem B 2005, 109, 11862.
15. Yang, Q. Y.; Zhong, C. L. J Phys Chem B 2006, 110, 655.
16. Sagara, T.; Klassen, J.; Ganz, E. J Chem Phys 2004, 121, 12543.
17. Sagara, T.; Klassen, J.; Ortony, J.; Ganz, E. J Chem Phys 2005, 123, 014701.
18. Hermes, S.; Schröter, M. K.; Schmid, R.; Khodeir, L.; Muhler, M.; Tissler, A.; Fischer, R. W.; Fischer, R. A. Angew Chem Int Ed Engl 2005, 44, 6237.
19. Kim, H.; Chun, H.; Kim, G.-H.; Lee, H.-S.; Kim, K. Chem Commun 2006, 2759.
20. Clark, L. A.; Snurr, R. Q. Chem Phys Lett 1999, 308, 155.
21. Leroy, F.; Rousseau, B.; Fuchs, A. H. Phys Chem Chem Phys 2004, 6, 775.
22. Vlugt, T. J. H.; Schenk, M. J Phys Chem B 2002, 106, 12757.
23. Forester, T. R.; Smith, W. Faraday Trans 1997, 93, 3249.
24. Li, H.; Eddaoudi, M.; O'Keeffe, M.; Yaghi, O. M. Nature 1999, 402, 276.
25. Clegg, W.; Harbron, D. R.; Homan, C. D.; Hunt, P. A.; Little, I. R.; Straughan, B. P. Inorg Chim Acta 1991, 186, 51.
26. Yin, M.-C.; Wang, C.-W.; Al, C.-C.; Yuan, L.-J.; Sun, J.-T. Wuhan Univ J Nat Sci 2004, 9, 939.
27. Becke, A. D. Phys Rev A 1988, 38, 3098.
28. Becke, A. D. J Chem Phys 1993, 98, 5648.
29. Lee, C.; Yang, W.; Parr, R. G. Phys Rev B 1988, 37, 785.
30. Dolg, M.; Wedig, U.; Stoll, H.; Preuss, H. J Chem Phys 1987, 86, 866.
31. Frisch, M. J.; Trucks, G. W.; Schlegel, H. B.; Scuseria, G. E.; Robb, M. A.; Cheeseman, J. R.; Montgomery, J. A., Jr.; Vreven, T.; Kudin, K. N.; Burant, J. C.; Millam, J. M.; Iyengar, S. S.; Tomasi, J.; Barone, V.; Mennucci, B.; Cossi, M.; Scalmani, G.; Rega, N.; Petersson, G. A.; Nakatsuji, H.; Hada, M.; Ehara, M.; Toyota, K.; Fukuda, R.; Hasegawa, J.; Ishida, M.; Nakajima, T.; Honda, Y.; Kitao, O.; Nakai, H.; Klene, M.; Li, X.; Knox, J. E.; Hratchian, H. P.; Cross, J. B.; Adamo, C.; Jaramillo, J.; Gomperts, R.; Stratmann, R. E.; Yazyev, O.; Austin, A. J.; Cammi, R.; Pomelli, C.; Ochterski, J. W.; Ayala, P. Y.; Morokuma, K.; Voth, G. A.; Salvador, P.; Dannenberg, J. J.; Zakrzewski, V. G.; Dapprich, S.; Daniels, A. D.; Strain, M. C.; Farkas, O.; Malick, D. K.; Rabuck, A. D.; Raghavachari, K.; Foresman, J. B.; Ortiz, J. V.; Cui, Q.; Baboul, A. G.; Clifford, S.; Cioslowski, J.; Stefanov, B. B.; Liu, G.; Liashenko, A.; Piskorz, P.; Komaromi, I.; Martin, R. L.; Fox, D. J.; Keith, T.; Al-Laham, M. A.; Peng, C. Y.; Nanayakkara, A.; Challacombe, M.; Gill, P. M. W.; Johnson, B.; Chen, W.; Wong, M. W.; Gonzalez, C.; Pople, J. A. Gaussian 03, Revision B.04; Gaussian: Pittsburgh, PA, 2003.
32. Weigend, F.; Häser, M.; Patzelt, H.; Ahlrichs, R. Chem Phys Lett 1998, 294, 143. Also available at ftp://ftp.chemie.uni-karlsruhe.de/pub/BASES/Def/def-TZVPP.
33. Wilson, A. K.; Woon, D. E.; Peterson, K. A.; Dunning, T. H. J Chem Phys 1999, 110, 7667.
34. Møller, C.; Plesset, M. S. Phys Rev 1934, 46, 618.
35. Raghavachari, K.; Trucks, G. W.; Pople, J. A.; Head-Gordon, M. Chem Phys Lett 1989, 157, 479.
36. Purvis, G. D. I.; Bartlett, R. J. J Chem Phys 1982, 76, 1910.
37. Watts, J. D.; Gauss, J.; Bartlett, R. J. J Chem Phys 1993, 98, 8718.
38. Schaftenaar, G.; Noordik, J. H. J Comput-Aided Mol Design 2000, 14, 123.
39. Ponder, J. W.; Richards, F. M. J Comput Chem 1987, 8, 1016. TINKER version 4.2, June 2004, (http://dasher.wustl.edu/tinker/).
40. Braga, C. F.; Longo, R. L. J Mol Struct (Theochem) 2005, 716, 33.
41. Johnson, M. K.; Powell, D. B.; Cannon, R. D. Spectrochim Acta A 1982, 38, 125.
42. Berkesi, O.; Andor, J. A.; Jayasooriya, U. A.; Cannon, R. D. Spectrochim Acta A 1992, 48, 147.
43. Head-Gordon, M.; Pople, J. A. J Phys Chem 1993, 97, 1147.
44. Hubner, O.; Gloss, A.; Fichtner, M.; Klopper, W. J Phys Chem A 2004, 108, 3019.
45. Besler, B. H.; Merz, K. M.; Kollman, P. A. J Comput Chem 1990, 11, 431.
46. Breneman, C. M.; Wiberg, K. B. J Comput Chem 1990, 11, 361.
47. Angyan, J.; Chipot, C.; Dehez, F.; Hattig, C.; Jansen, G.; Millot, C. J Comput Chem 2003, 24, 997.
48. Sigfridsson, E.; Ryde, U. J Comput Chem 1998, 19, 377.
49. Stone, A. J. J Chem Theor Comput 2005, 1, 1128.
50. Allinger, N. L.; Zhou, X. F.; Bergsma, J. J Mol Struct (Theochem) 1994, 118, 69.
51. Bayly, C. L.; Cieplak, P.; Cornell, W. D.; Kollman, P. A. J Phys Chem 1993, 97, 10269.
52. Ermoshin, V. A.; Smirnov, K. S.; Bougeard, D. Chem Phys 1996, 202, 53.
53. Sipachev, V. A. J Mol Struct (Theochem) 1985, 121, 143.
54. Allinger, N. L.; Yuh, Y. H.; Lii, J.-H. J Am Chem Soc 1989, 111, 8551.
55. Allinger, N. L.; Li, F.; Yan, L.; Tai, J. C. J Comput Chem 1990, 11, 868.
56. Vaiana, A. C.; Cournia, Z.; Costescu, I. B.; Smith, J. C. Comput Phys Commun 2005, 167, 34.
57. Fuentes-Cabrera, M.; Nicholson, D. M.; Sumpter, B. G.; Widom, M. J Chem Phys 2005, 123, 124713.
58. Mattesini, M.; Soler, J. M.; Yndurain, F. Phys Rev B 2006, 73, 094111.
59. Mueller, T.; Ceder, G. J Phys Chem B 2005, 109, 17974.
60. Mulder, F. M.; Dingemans, T. J.; Wagemaker, M.; Kearley, G. J. Chem Phys 2005, 317, 113.
61. Civalleri, B.; Napoli, F.; Noel, Y.; Roetti, C.; Dovesi, R. Cryst Eng Commun 2006, 8, 364.
62. Bornhauser, P.; Bougeard, D. J. J Phys Chem B 2001, 105, 36.
63. Hermes, S.; Schröter, F.; Amirjalayer, S.; Schmid, R.; Fischer, R. A. J Mater Chem 2006, 16, 2464.
64. Stallmach, F.; Gröger, S.; Künzel, V.; Kärger, J.; Yaghi, O. M.; Hesse, M.; Müller, U. Angew Chem Int Ed Engl 2006, 45, 2123.
65. Amirjalayer, S.; Tafipolsky, M.; Schmid, R. Angew Chem Int Ed Engl 2007, 46, 463.